1

2 # Design of a novel membrane-integrated waste acid recovery

3 # process from pickling solution

4

5 **A. Culcasi, R. Gueccia, S. Randazzo*, A. Cipollina, G. Micale**

6 *Dipartimento di Ingegneria, Università di Palermo – Viale delle Scienze ed.6, 90128 Palermo, Italy*
7 *Corresponding author: Tel: +3909123863779; E-mail: serena.randazzo@unipa.it*
8

9 **Abstract**

10 Hydrochloric acid pickling is a common practice in steel manufacturing industry. During the process,

11 acid is consumed to dissolve surface oxides and metals ions are accumulated in the solution, which

12 becomes less effective with time. In addition, the costly and risky waste acid disposal is another issue

13 affecting the hot-dip galvanizing industry.

14 In this work, a novel sustainable waste acid recovery process from pickling solutions based on

15 circular approach is proposed to tackle these issues. The innovative system allows (i) the continuous

16 regeneration of pickling solutions to enhance process rate and performance and (ii) minimise the

17 highly expensive and environmentally risky wastewater disposal. In this way, refilling pickling baths

18 with fresh acid, as done in conventional operation, can be avoided and can be carried out continuously

19 under optimal working conditions. Moreover, the recovery of valuable substances (e.g. metal

20 hydroxide or salts solution) can be obtained as an additional benefit. Continuous treatment and

21 regeneration of pickling solution can be accomplished by coupling diffusion dialysis (DD) and

1 membrane distillation (MD) technologies with a reactive precipitation unit where iron ions can be

2 separated from the zinc-rich solution, in order to recover valuable products.

3 To this purpose, a steady state process simulator was developed to predict the operation of the

4 proposed integrated process.

5 **Keywords**: Process simulator; Industrial wastewater; Ion-Exchange membranes; Hydrochloric acid

6 concentration; Steel manufacturing

7

1. Introduction

The pickling process is an essential step in the hot-dip galvanizing process as the surface of manufactured steel pieces is cleaned from the oxidized layers. In fact, during hot-dip galvanization, the manufactured steel pieces are immersed in a molten zinc bath, thus a good pickling is important in order to achieve a more uniform contact surface. The dissolution of the oxidized metal layers is obtained by immersing manufactured steel pieces in acid baths. During the pickling process, acid attacks metal oxides on the surface, dissolving them in the pickling bath. Thus, the efficiency of the pickling liquor decreases due to the accumulation of metal ions and the consumption of free acid in the solution (Kleingarn, 1988). When hydrochloric acid is used, ferrous chloride is produced during the pickling treatment, reaching Fe^{2+} concentrations up to 200-250 g l^{-1}, while the acid concentration decreases by 75-85%. A pickling bath in this condition is considered spent (Regel-Rosocka, 2010) due to the very low pickling rate, hence it needs to be replaced. In common industrial practice, part of the exhausted solution is withdrawn and replaced with fresh acid to prolong the pickling bath life, while spent solution is disposed as a waste. Disposal of the spent pickling solution strongly affects the hot-dip galvanizing industries environmental footprint and costs. Thereby, a cleaner pickling process could be one of the most beneficial steps to achieve a sustainable development of hot-dip galvanizing industry (Kong and White, 2010). In fact, for instance, by their holistic approach adopted to assess hot-dip galvanizing process sustainability, Hernandez-Betancur et al. found that pickling stage is critical and it is not expected to be improved without a significant modification of the process (Hernández-Betancur, 2019). The remarkable importance of this step in hot-dip galvanizing industry have significantly boosted the interest of researchers and technologists.

Some researchers studied strategies to apply the zero emission/discharge concept to improve pickling process by identifying optimisation options, yet maintaining conventional equipment (Fresner et al., 2007). Others focused on the pickling rate optimization by using an optimal iron/hydrochloric acid concentration ratio in the pickling tank aiming at the minimization of waste acid (Stocks et al., 2005).

3

1 A different and likely more effective approach is to recover waste acid solutions by means of

2 auxiliary technologies.

3 A conventional method for the disposal of the waste acid solution is the direct discharge after

4 neutralization by common alkaline reactants. Up to now, several other methods to *recover* acid from

5 spent pickling solutions have been developed such as the combination of crystallization and

6 evaporation (Leonzio, 2016), distillation combined with solvent extraction or crystallization

7 (Machado et al., 2017) or more innovative membrane separation methods as the Diffusion Dialysis

8 (Xu et al., 2009). As far as the *regeneration* of HCl is concerned, the spray roasting (the so-called

9 "Ruthner process") and the fluidized bed processes (the so-called KCH technology) are applied at

10 the industrial scale in many plants in the world (Bascone et al., 2016).

11 In the present work, a novel sustainable process to recover waste acid from pickling solutions is

12 proposed. For the first time, a circular economy approach is applied in the hot-dip galvanizing

13 industry. The innovative system allows (i) the continuous regeneration of the pickling solutions

14 enhancing the pickling rate and process performance, (ii) the recovery of valuable compounds (e.g.

15 acid and metals) and (iii) the significant reduction of the industrial wastewater disposal. This goal

16 can be achieved by integrating a reactive precipitation unit with two different cutting-edge membrane

17 technologies (i.e. diffusion dialysis and membrane distillation). Membrane techniques are considered

18 simple, effective and sustainable and can be easily scaled from small to medium size installations

19 (Regel-Rosocka, 2010).

20 Diffusion dialysis (DD) is a simple membrane separation technique, which can be successfully used

21 for the treatment of waste acid solutions containing very high concentrations of metal ions. Thanks

22 to the anionic exchange membrane used in the DD module, separation of acid and metal salts occurs

23 (Palatý and Bendová, 2009). Many authors have reported promising results so far for the recovery of

24 HCl with DD. In particular, research efforts have been devoted to analysing how the acid

25 concentration and the presence of metal salts (e.g. $FeCl_2$ and $ZnCl_2$) can affect HCl recovery in DD.

26 In fact, chloride ions permeability is affected by the metal chloride involved in the process. Iron salt

enhances HCl diffusion through the membrane due to the so-called "salt effect", because of the supply of Cl$^-$ ions (Luo et al., 2013). However, even an iron leakage occurs and this phenomena increases as the iron ion concentration increases (Xu et al., 2009). Conversely, zinc ions reduce HCl diffusion due to the formation of negatively-charged zinc chloro-complexes (Jung Oh et al., 2000; Palatý and Žáková, 2006).

Membrane distillation (MD) can be used to concentrate hydrochloric acid solutions (Liu et al., 2012). A hydrophobic membrane separates two aqueous solutions at different temperature and composition. The different partial pressures at the two membrane sides generate the driving force for the passage of vapour molecules through the microporous membrane and the permeate composition is a function of both the temperature and the composition of the feed (Tomaszewska et al., 2001). Interestingly, the process can be performed at a feed temperature considerably lower than its boiling point, thus allowing the utilization of waste heat or alternative thermal energy sources (Tomaszewska et al., 2001).

The novel integrated process proposed in the present work was investigated by developing a steady state process simulator able to predict its operation. Moreover, a parametric analysis of the process was performed by evaluating the effect of the inlet stream (pickling solution) composition on the process performance figures of merit (e.g. recovery ratio, concentration ratio, etc.). The analysis here presented refers to a specific case study, relevant to a real hot-dip galvanizing plant.

It is worth noting that the final aim of the present work will be to support the design, construction and operation of a pilot system, final goal of the EU-funded ReWaCEM project aiming at: "*reducing water use, wastewater production, energy use, valuable metal resource recovery and water footprint by between 30-90% in the metal plating, galvanizing and printed circuit board industry*".

1   **2. Processes description**

2   In this section, the main steps of the hot-dip galvanizing process are analysed with particular focus

3   on pickling. Moreover, the proposed integrated process is described in detail.

4   **2.1 Pickling process: main facts**

5   The hot-dip galvanizing process is an industrial technique that allows the corrosion protection of the

6   manufactured steel. Hot-dip galvanizing process includes several steps. Figure 1 reports the process

7   of the Tecnozinco Co. plant, located in Italy. Following the pathway shown, the manufactured steel

8   is first degreased in a bath under the emulsifying action of surfactants, namely non-ionic surfactants,

9   for oil removal. Then, the pickling process occurs. After that, the manufactured steel pieces are

10   washed in a rinsing tank to remove residual acidic solution. Finally, they are put in a fluxing bath

11   before being dried and galvanized (i.e. immersed in the molten zinc bath).
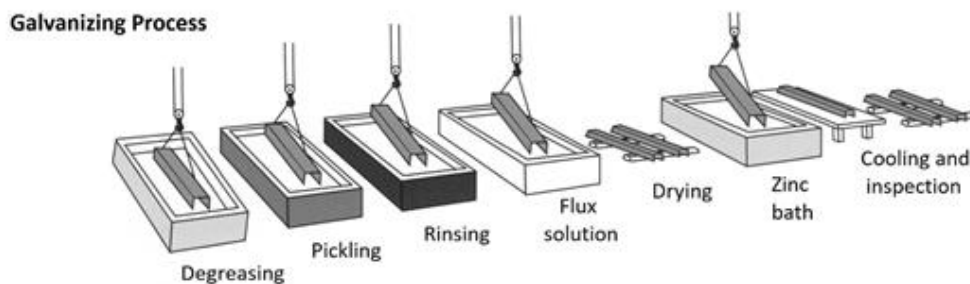

12

13   **Figure 1.** Sketch of the hot-dip galvanizing process steps at Tecnozinco Co. plant adapted from
14   https://galvanizeit.org/hot-dip-galvanizing/what-is-galvanizing/hdg-process

15   The fluxing solution contains zinc and ammonium salts to protect the manufactured steel during the

16   drying process and before the immersion in the molten zinc bath and to catalyse zinc covering in this

17   latter step. Steel pickling is typically performed by immersing the manufactured steel in hydrochloric

18   acid (HCl) bath. The kinetic of pickling chemical reactions is strongly affected by the presence of acid

19   molecules and the iron ions concentration. A specific relationship between the acid and the iron

20   concentration for optimal pickling operation is reported in the literature and known as the *Kleingarn*

1 *Curve* (Kleingarn, 1988). In Figure 2, the optimal pickling line and the delimited pickling active region

2 are reported. In addition, also the composition of some representative samples from Tecnozinco pickling

3 baths are shown in the Figure 2. Therefore, controlling acid and iron concentrations within the tank

4 increases pickling rate compared to replacing the entire spent acid bath with fresh acid.

5
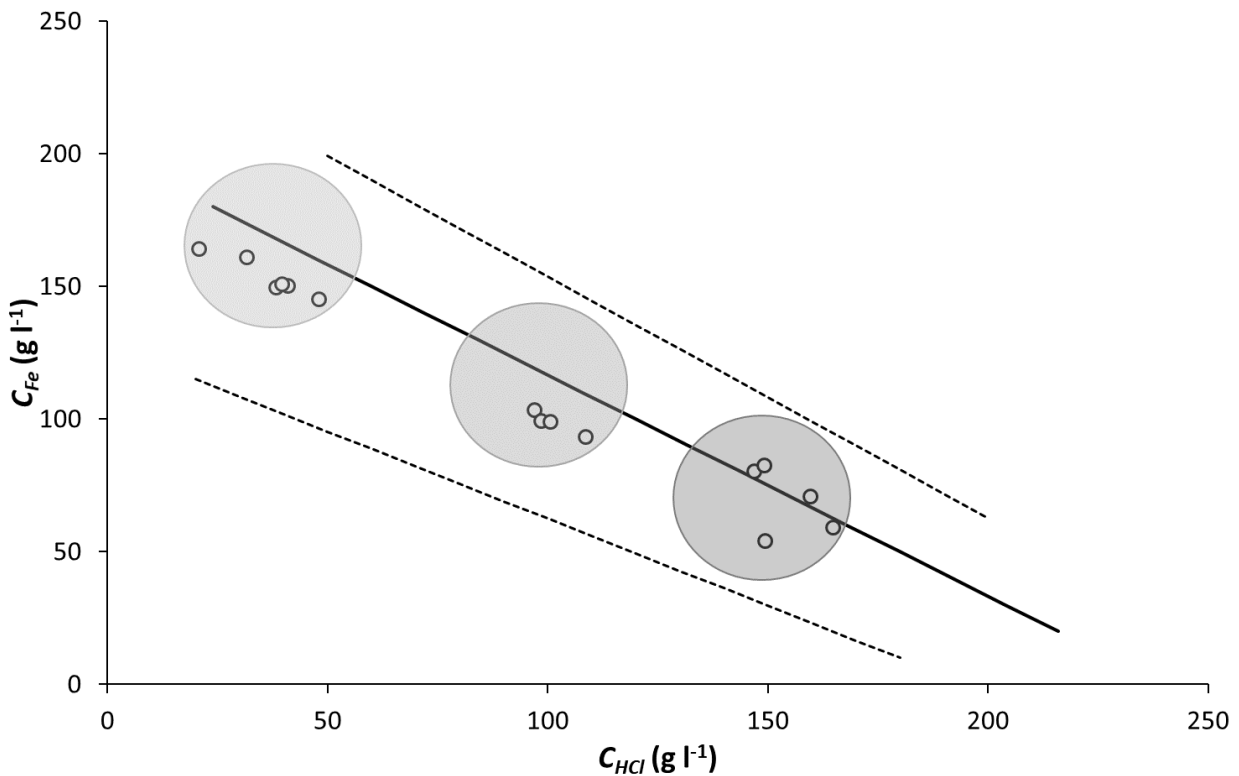
Figure 2. Graphical representation of the optimal pickling Kleingarn curve (continuous line) (Kleingarn, 1988), with indication of minimum and maximum threshold lines for pickling operation (dashed lines). Empty circles represent the compositions of some real samples from Tecnozinco pickling baths.

9 Tecnozinco facility uses 7 pickling bathes containing in total more than 350 m³ of acid pickling solution.

10 The site has a capacity of 20,000 tons per year of treated steel. The acid consumption is approximately

11 160-240 ton per year. Bathes can be grouped in three classes according to the "pickling power": highly

12 effective pickling at higher acid concentration and lower iron concentration (HCl 125-170 g l⁻¹, Fe 40-

13 100 g l⁻¹ - area A in Figure 2), intermediate effective pickling at intermediate acid and iron

14 concentrations (HCl 75-120 g l⁻¹, Fe 80-145 g l⁻¹ - area B in Figure 2) and poorly effective pickling at

15 lower acid concentration and higher iron concentration (HCl 15-60 g l⁻¹, Fe 135-195 g l⁻¹ - area C in

1 Figure 2). Based on periodical analysis of free acidity and iron content, the pickling solution composition

2 is "adjusted" by spilling part of the solution and subsequent replenishing with water and HCl in order to

3 remain close to the optimal condition curve.

4 Besides iron ions, also zinc is present in the pickling tanks of hot-dip galvanizing plants where goods

5 and winches used for pieces handling are often covered with zinc. Therefore, the pickling process

6 generates a waste acid stream of approximately 300 ton per year, characterized by high concentrations

7 of heavy metals, namely iron (150-180 g l^{-1}) and zinc (10-30 g l^{-1}). Disposal costs incurred by

8 Tecnozinco represent an important cost item. In fact, in addition to dispose, also transportation to a waste

9 treatment plant located in northern Italy has to be considered. The total disposal cost is around 0.16 €/kg,

10 of which 50% for the transport. Of course, reducing waste would reduce (i) disposal costs, (ii) operators'

11 labor for the handling of large quantity of such environmentally risky wastewater and (iii)

12 environmental pollution due to the road transport.

13 **2.2 Integrated process description**

14 The proposed innovative process aims at integrating DD and MD processes with a reactive precipitation

15 unit to keep HCl and iron concentrations in the pickling tank at the optimal values and to separate iron

16 and zinc ions in a reactive precipitation unit producing two valuable by-product streams.

17 The Process Flow Diagram and relative streams characterization are shown in Figure 3.

18 The outgoing stream from the pickling tank, named *Waste Acid solution (WAS),* is pre-treated in order

19 to remove particles, oil and surfactants. Then, it is fed to the Diffusion Dialysis unit (in the retentate

20 side) where the recovery of acid occurs. Here, a high percentage of the acid (around 80%) is recovered

21 from the waste solution thanks to the anionic exchange membrane, which allows the transport of

22 chlorides driven by a concentration difference to the diffusate compartment, while rejecting large cations

23 in solution. Thanks to their small size and high mobility, H^+ ions can diffuse through the anionic

24 membrane, by means of the so-called tunneling mechanism (Luo et al., 2011). Therefore, the acid is

25 recovered in the diffusate side of the DD unit and separation from salts occurs. An ideal membrane

8

1   should reject 100% of metal ions, in practice, real Anionic Exchange Membranes (AEMs) allow some

2   iron and zinc ions to diffuse through them, reaching leakage percentage of 5-10% for iron and up to 50-

3   60% for zinc (Xu et al., 2009). This latter can be actually explained due to the formation of negative

4   Zn^{2+} complexes in solution as $ZnCl_3^-$ and $ZnCl_4^{2-}$, whose diffusion through AEMs is allowed.

5
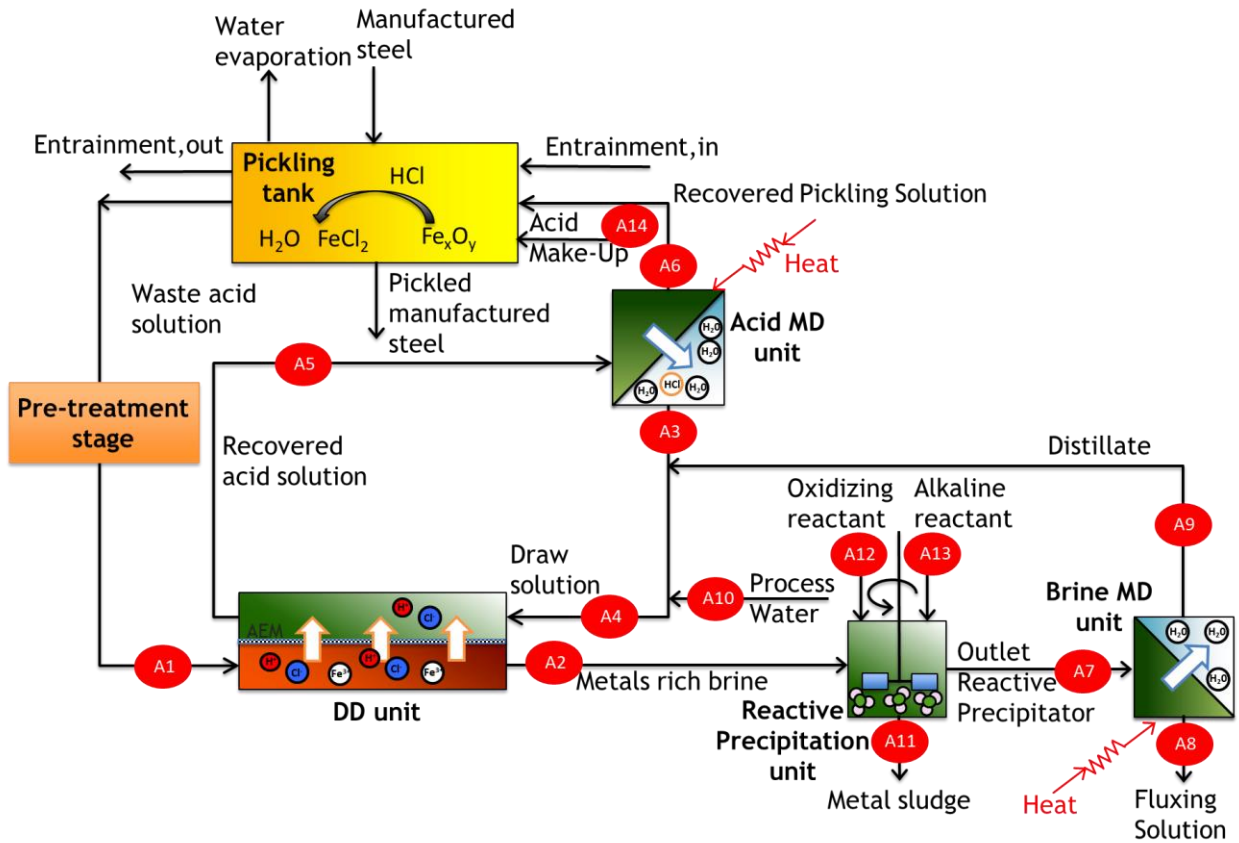
6

7   **Figure 3.** Process Flow Diagram (PFD) of the membrane-integrated process for HCl and metals
8   recovery. Red circles identify all main process streams.

9   The stream enriched in acid, named *Recovered Acid Solution (RAS)* is sent to the Membrane Distillation

10   (MD) unit, where the acid is concentrated by evaporation/removal of water. In the MD unit, the

11   microporous hydrophobic membrane separates two aqueous solutions at different temperature and

12   composition: the *RAS,* enriched in acid, in the hot side and the *Permeate*, mainly distilled water, in the

13   cold side. In fact, the membrane rejects liquid solution and permits vapour passage from the hot to the

14   cold side. Thus, mainly water vapour passes and condenses directly in the *Permeate* stream within the

1 cold compartment. As a drawback, also HCl can pass from the feed to the vapour phase and is

2 transported through the membrane especially at high concentrations (Tomaszewska et al., 1995).

3 The *Permeate* stream from MD is blended with two streams of water, i.e. *Distillate* from Brine MD unit

4 and *Process Water (PW),* used as a feed drawing solution to the DD unit (diffusate side), namely the

5 *Draw Solution (DS)*. The stream exiting from MD feed channel, the concentrated *Recovered Pickling*

6 *Solution (RPS)*, is finally sent to the pickling tank.

7 The other stream exiting from the DD unit in the retentate side, called *Metals Rich Brine (MRB)*, is a

8 low-acid ($0<pH<1$) stream enriched in iron and zinc chlorides. This stream is fed to the Reactive

9 Precipitation unit where the acid is neutralized and iron hydroxide is produced by addition of ammonia

10 solution. Moreover, a hydrogen peroxide stream is added since the iron in solution is mainly present

11 in reduced form (Fe(II)). Here, oxidizing process is necessary to obtain a highly pure iron hydroxide

12 precipitate, free of zinc. In fact, pH precipitation of zinc hydroxide is very similar to iron(II)

13 hydroxide, but higher enough than that of iron(III) hydroxide to obtain the precipitation of only

14 iron(III) at an operating pH range of 3-4. As a consequence, a zinc chloride/ammonium chloride

15 solution is produced from this stage, the *Outlet Reactive Precipitator* stream *(ORP).* Moreover, iron

16 hydroxide precipitates within the reactor and the resulting *Metal Sludge (MS)* can be treated in a filter

17 press to recover iron hydroxide as a product. Finally, the *ORP* salty stream is concentrated in a Brine

18 Membrane Distillation unit where water is produced as *Distillate* stream. The Brine MD outlets, the

19 *Fluxing Solution* and the *Distillate*, can be suitably re-used in the fluxing bath of the hot-dip galvanizing

20 plant and as process water in the integrated process, respectively.

21 In order to compensate the acid reacted in the pickling bath and that lost in the *MRB*, a *Make-Up (MU)*

22 of fresh acid is needed in the pickling bath to maintain the optimal concentration.

23 The above-described integrated scheme is a nice example of a sustainable process integration and raw

24 materials use, in which all process streams are recirculated in order to re-use a waste stream from a unit

25 as a feed for another or, more in general, to re-use a produced stream elsewhere in the plant or

26 commercializing it. Thus, an overall recovery of materials and minimization of waste streams can be

1 successfully achieved. Moreover, for the pilot-scale unit installed at Tecnozinco, a recovery of waste

2 heat, necessary for the MD operation, is also planned for enhancing the process sustainability.

3. Modeling the integrated process

4 A mathematical model able to simulate the integrated system operations was developed and

5 implemented in Microsoft® Office Excel spreadsheets with Macros in Visual Basic language.

6 Hereinafter, model details are presented for each unit.

3.1 Pickling unit

8 The first step of the modeling activity was to fix parameters and operative conditions of the pickling

9 process.

3.1.1 Data mining from Tecnozinco plant

11 In order to estimate the reaction rate of each chemical compound within the pickling tank, two possible

12 options are possible: using kinetics data from literature or collecting information from available

13 historical statistics of the company. In this work, the latter was selected as starting point using average

14 data of the last 5 years. To this purpose, streams reported in Figure 4 were considered and the real data

15 collected from Tecnozinco for a manufactured steel flow rate of 7,410 ton y^{-1}, fixing a time frame of 1
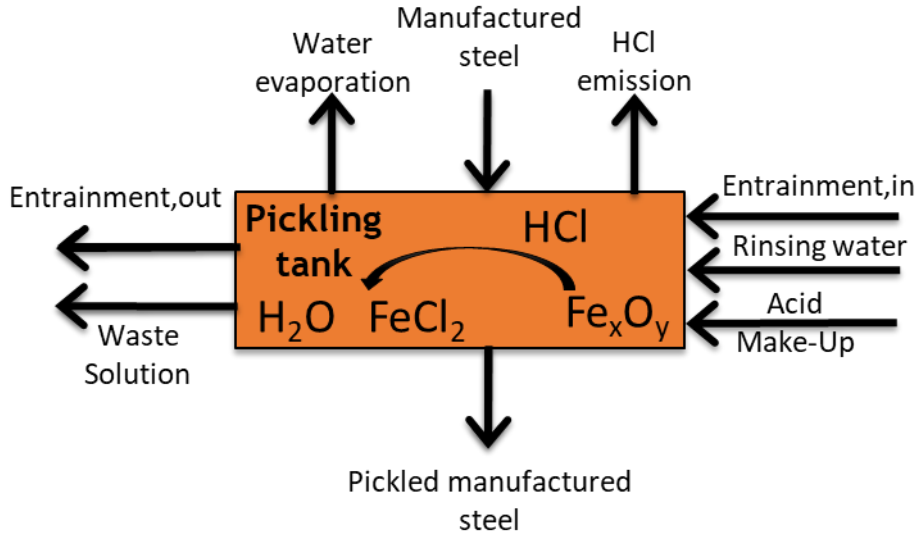
16 year, are shown in Table 1.

Figure 4. Scheme of the pickling process at Tecnozinco plant.

Table 1. Operational data on inlet/outlet streams under "traditional" operation of Tecnozinco plant

	Acid Make-Up	Waste Solution	Rinsing water	Entrainment Inlet	Entrainment Outlet	HCl emission	Water evaporation
	173 ton y^{-1}	247 ton y^{-1}	48.1 ton y^{-1}	2.5 l ton^{-1}	2.5 l ton^{-1}	0.33 ton y^{-1}	4.2 kg ton^{-1}
C_{HCl}	400 g l^{-1}	8.50 g l^{-1}	16 g l^{-1}	0.00 g l^{-1}	97 g l^{-1}	-	-
ρ	1,170 g l^{-1}	1,296 g l^{-1}	1,087 g l^{-1}	1,092 g l^{-1}	1,254 g l^{-1}	-	-

The chemical pickling reactions considered in the presence of corrosion inhibitors are reported in

Equations (1) and (2) (Jatuphaksamphan et al., 2010)

$$Fe_2O_3 + Fe + 6HCl = 3FeCl_2 + 3H_2O \tag{1}$$

$$Fe_3O_4 + Fe + 8HCl = 4FeCl_2 + 4H_2O \tag{2}$$

Reaction (1) accounts for the 20% and reaction (2) for the 80% of the overall acid consumption

according to the average metal scale composition (Campano, 2012). Depending on the HCl consumed

per year (reported in Table 1), the reaction rate of the hydrochloric acid follows the expression

$$k_{HCl} = \frac{10^3 \cdot \left(w_{y,HCl}^{MU} + w_{y,HCl}^{Rinsing} + w_{y,HCl}^{entr,in} - w_{y,HCl}^{entr,out} - w_{y,HCl}^{waste} - w_{y,HCl}^{gas} \right)}{N_{hours}} \tag{3}$$

1 where $w_{y,HCl}^{MU}$, $w_{y,HCl}^{Rinsing}$, $w_{y,HCl}^{entr,in}$, $w_{y,HCl}^{entr,out}$, $w_{y,HCl}^{waste}$ and $w_{y,HCl}^{gas}$ are the make-up, the rinsing, the

2 entrainment inlet, the entrainment outlet, the actual waste produced in Tecnozinco and the gaseous

3 emission of HCl flow rate, respectively. N_{hours} is the number of yearly working hours equal to 3,650.

4 The rate of consumed oxides and of released iron ions, water and chloride ions from the complexation

5 reactions reported in Equations (1) and (2), can be quantified as follows:

$$k_{oxides} = 0.2 \cdot \frac{k_{HCl}\left(MM_{Fe_2O_3}+MM_{Fe}\right)}{6\ MM_{HCl}} + 0.8 \cdot \frac{k_{HCl}\left(MM_{Fe_3O_4}+MM_{Fe}\right)}{8\ MM_{HCl}} \qquad (4)$$

$$k_{Fe} = \frac{k_{HCl}\ MM_{Fe}}{2\ MM_{HCl}} \qquad (5)$$

$$k_w = \frac{k_{HCl}\ MM_w}{2\ MM_{HCl}} \qquad (6)$$

$$k_{Cl} = \frac{k_{HCl}\ MM_{Cl}}{MM_{HCl}} \qquad (7)$$

6 Estimated kinetic constants values are reported in Table 2.

7 **Table 2.** Kinetic constants values for the components involved in reactions (1) and (2)

k_{HCl} (kg h^{-1} ton^{-1})	7.6	HCl consumption per ton of steel manufactured
k_{oxides} (kg h^{-1} ton^{-1})	7.5	Oxides and iron consumption per ton of steel manufactured
k_{Fe} (kg h^{-1} ton^{-1})	5.8	Iron ions released per ton of steel manufactured
k_w (kg h^{-1} ton^{-1})	1.9	Water released per ton of steel manufactured
k_{Cl} (kg h^{-1} ton^{-1})	7.4	Chloride ions released per ton of steel manufactured

8 *3.1.2 Pickling unit modeling*

9 For the modeling of the pickling tank, the streams considered are shown in Figure 5: *Manufactured*

10 *Steel*, *Entrainment,in,* Acid *Make-Up* and *Recovered Pickling Solution* as inlets, *Waste Acid Solution*,

11 *Entrainment,out, Water evaporation* and *Pickled Manufactured Steel* as outlets.

13
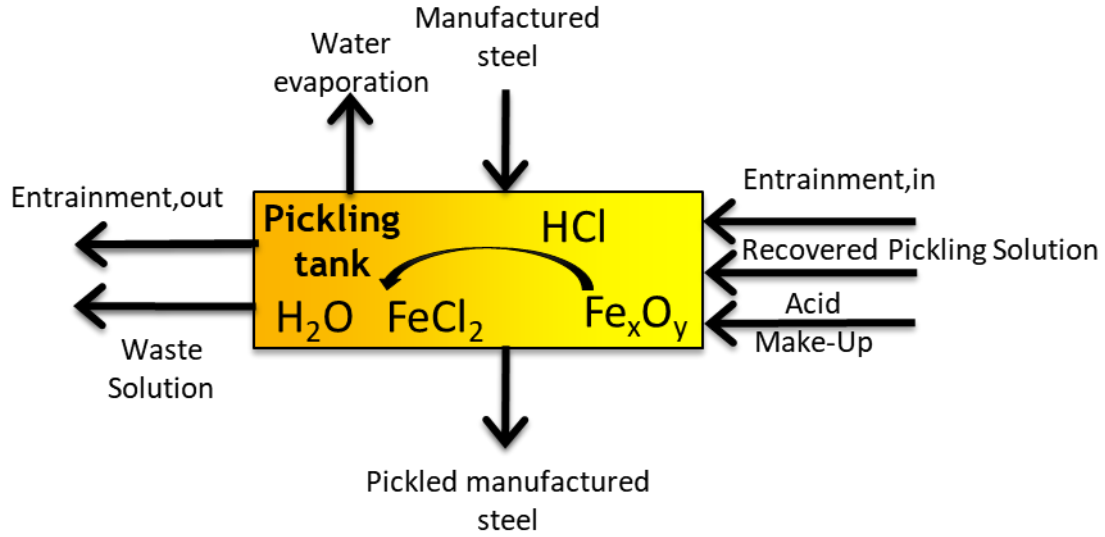
Figure 5. Pickling process scheme.

The pickling bath is modeled as a continuous stirred-tank reactor (CSTR) and the pickled manufactured

steel is fixed equal to 290 kg per working hour. As a result, the volumetric flow rate coming from the

pickling bath is calculated by Eq. 8:

$$F^{WAS} = \frac{k_{Fe} \cdot m_s + w_{Fe}^{DD} + w_{Fe}^{entr,in} - w_{Fe}^{entr,out}}{10^{-3} \cdot C_{Fe}^{WAS}} \tag{8}$$

where F^{WAS} is the *Waste Acid Solution* volumetric flow rate, k_{Fe} is the iron release rate, m_s is the

pickled manufactured steel mass, w_{Fe}^{DD} is the iron mass flow rate arriving with the acid from the whole

recovery process, $w_{Fe}^{entr,in}$ and $w_{Fe}^{entr,out}$ are the iron flow rates related to the streams *Entrainment,in*

and *Entrainment,out* arriving from the degreasing and leaving to the rinsing tanks, respectively. C_{Fe}^{WAS}

represents the optimal iron concentration corresponding to the optimal HCl concentration of the pickling

process, calculated from the Kleingarn Curve (see Figure 2), as reported in Eq. 9:

$$C_{Fe} = -0.833 \cdot C_{HCl} + 200 \tag{9}$$

To evaluate the process streams mass density, the model developed by Lalibertè et al. was adopted

(Lalibertè and Cooper, 2004). As the tank is considered as a CSTR, the *Waste Acid Solution*

composition is constant during the process and it is equal to the composition inside the pickling tank.

1 The mass flow rate of the Acid *Make-Up* stream is calculated by the following equation:

$$w_{HCl}^{MU} = w_{HCl}^{MRB} + k_{HCl} \cdot m_s + w_{HCl}^{entr,out} \tag{10}$$

2 where w_{HCl}^{MU}, w_{HCl}^{MRB} and $w_{HCl}^{entr,out}$ are the hydrochloric acid mass flow rates of the *Make-Up, Metals*

3 *Rich Brine* and *Entrainment,out* streams, respectively. The $k_{HCl} \cdot m_s$ term concerns the HCl flow

4 rate reacted in the pickling process.

5 To complete the estimation of the main streams of the integrated system, *Process Water* stream is

6 evaluated by performing a global mass balance using the entire integrated system as control volume

7 (Eq. 11).

$$w^{pw} = w^{MRB} + w^{entr,out} + w^{evap} - w^{MU} - k_{oxides} \cdot m_s - w^{entr,in} \tag{11}$$

8 where $w^{pw}, w^{MRB}, w^{entr,out}, w^{evap}, w^{MU}$ and $w^{entr,in}$ are the water mass flow rates in the *Process*

9 *Water* incoming into the system, in the *Metals Rich Brine*, in the *Entrainment,out*, in the evaporation,

10 in the *Make-Up* and in the *Entrainment,in* streams, respectively. The $k_{oxides} \cdot m_s$ term concerns the

11 oxides mass flow rate inlet within the manufactured steel in the pickling tank.

12 **3.2 Diffusion Dialysis unit**

13 Concerning the Diffusion Dialysis unit, the streams considered for the integrated process simulation

14 are: *Waste Acid Solution* and *Draw Solution* as inlets, *Recovered Acid Solution* and *Metals Rich Brine*

15 as outlets (see Figure 6).
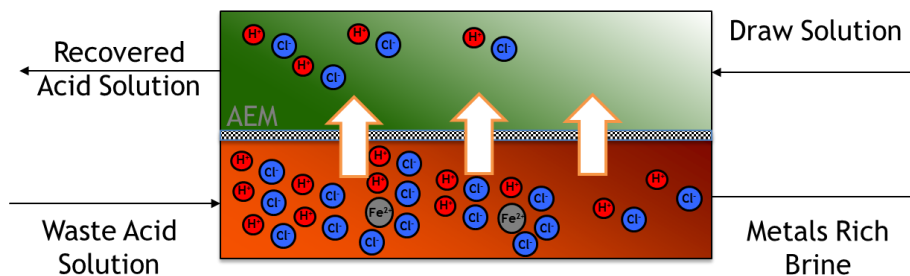
16

17 **Figure 6.** Diffusion dialysis process scheme.

18 The ratio between *WAS* and *DS* volumetric flow rates is assumed fixed to 1.

1 The equations used in this section were derived from the results obtained from an experimental

2 investigation carried out by some of co-authors (Gueccia et al., 2019a). Experiments were performed

3 with a DD laboratory test-rig, where a Fumatech FAD-type Anionic Exchange Membrane (AEM)

4 was adopted, in order to collect information for calibrating/validating the model before using it for

5 design purposes.

6 The hydrochloric acid recovery was obtained by using Eq. 12, based on a lumped-parameters

7 mathematical description of the DD unit:

$$w_{HCl}^{DD} = A \cdot \left(P_{HCl} \cdot \left(\overline{C_{HCl}^{R}} - \overline{C_{HCl}^{D}} \right) + 3{,}600 \cdot MM_{HCl} U_{HCl}^{FeCl_2} \left(\overline{C_{Fe,mol}^{R}} - \overline{C_{Fe,mol}^{D}} \right) \right.$$
$$\left. - 3{,}600 \cdot MM_{HCl} U_{HCl}^{ZnCl_2} \left(\overline{C_{HCl,mol}^{R}} - \overline{C_{HCl,mol}^{D}} \right) \right) \tag{12}$$

8 where w_{HCl}^{DD} is the mass flow rate of hydrochloric acid passing from the retentate to the diffusate side

9 of the DD unit, A is the membrane area, MM_{HCl} is the HCl molar mass, P_{HCl} is the membrane

10 permeability to hydrochloric acid and $U_{HCl}^{FeCl_2}$, $U_{HCl}^{ZnCl_2}$ are the secondary overall mass transfer

11 coefficient taking in account the passage of acid due to the presence of the chlorides salts. $\overline{C_{HCl}^{R}}$ and

12 $\overline{C_{HCl}^{D}}$ are the average mass concentrations of hydrochloric acid in the retentate and diffusate side

13 respectively, $\overline{C_{HCl,mol}^{R}}$, $\overline{C_{HCl,mol}^{D}}$ and $\overline{C_{Fe,mol}^{R}}$, $\overline{C_{Fe,mol}^{D}}$ are the average molar concentrations of

14 hydrochloric acid and iron in the retentate and in diffusate side, respectively. The expressions for

15 P_{HCl}, $U_{HCl}^{FeCl_2}$ and $U_{HCl}^{ZnCl_2}$ were derived experimentally (Gueccia et al., 2019a; Gueccia et al., 2019b)

16 and are reported in Eqs. 13 - 15.

$$P_{HCl} = 1.16 \cdot 10^{-3} \overline{C_{HCl,mol}^{R}}^{3} - 6.95 \cdot 10^{-3} \overline{C_{HCl,mol}^{R}}^{2} + 1.48 \cdot 10^{-2} \overline{C_{HCl,mol}^{R}} + 2.38 \cdot 10^{-3} \tag{13}$$

$$^{*}U_{HCl}^{FeCl_2} = 2.00 \cdot 10^{-6} \cdot \overline{C_{HCl,mol}^{R}} + 3.47 \cdot 10^{-7} \tag{14}$$

---

* Eqs. 14 and 17 adapted from (Gueccia et al., 2019a), including some further implementation on the basis of new experiments in the presence of Zn that affect the parameter

$$U_{HCl}^{ZnCl} = 6.09 \cdot 10^{-5} \cdot \overline{C_{Zn,mol}^R}^2 - 8.50 \cdot 10^{-5} \cdot \overline{C_{Zn,mol}^R} + 2.83 \cdot 10^{-5} \qquad (15)$$

1   in which $\overline{C_{HCl,mol}^R}$ and $\overline{C_{Zn,mol}^R}$ are the hydrochloric acid and zinc molar average concentration in the

2   retentate side.

3   Although the anionic exchange membrane theoretically rejects all iron cations, a small passage of

4   iron chloride is observed (Gueccia et al., 2019a). Therefore, salt diffusion through the AEM

5   membrane was considered by Eq. 16.

$$w_{Fe}^{DD} = 0.7 \cdot A \cdot P_{Fe} \cdot \left(\overline{C_{Fe,mol}^R} - \overline{C_{Fe,mol}^D} \right) \qquad (16)$$

6   where w_{Fe}^{DD} is the iron mass flow rate passing from the retentate to the diffusate side of the DD unit,

7   A is the membrane area, P_{Fe} is the membrane permeability to the FeCl$_2$, MM_{Fe} is the Fe molar mass,

8    $\overline{C_{Fe,mol}^R}$ and $\overline{C_{Fe,mol}^D}$ are the iron average concentrations in the retentate and in the diffusate side,

9   respectively. The expression for P_{Fe} was derived experimentally (Gueccia et al., 2019a) and it is

10   reported in Eq. 17.

$$^*P_{Fe} = -8.97 \cdot 10^{-5} \cdot \overline{C_{Fe,mol}^R}^2 + 5.43 \cdot 10^{-4} \cdot \overline{C_{Fe,mol}^R} + 1.39 \cdot 10^{-3} \qquad (17)$$

11   in which $\overline{C_{Fe,mol}^R}$ is the average iron molar concentration in the retentate side of the DD unit.

12   Concerning the zinc passage, the following equation 18 was adopted:

$$w_{HCl}^{DD} = A \cdot \left(P_{Zn} \cdot \left(\overline{C_{Zn}^R} - \overline{C_{Zn}^D} \right) + 3,600 \cdot MM_{Zn} U_{ZnCl_2}^{FeCl_2} \left(\overline{C_{Fe,mol}^R} - \overline{C_{Fe,mol}^D} \right) \right.$$
$$\left. + 3,600 \cdot MM_{Zn} U_{ZnCl_2}^{FeCl_2} \left(\overline{C_{HCl,mol}^R} - \overline{C_{HCl,mol}^D} \right) \right) \qquad (18)$$

13   where w_{Zn}^{DD} is the zinc mass flow rate across the AEM, A is the membrane area, $\overline{C_{Zn}^R}$ and $\overline{C_{Zn}^D}$ are the

14   zinc mass concentration in the retentate and diffusate side respectively, $\overline{C_{Fe,mol}^R}$ and $\overline{C_{HCl,mol}^R}$ are the

15   iron and hydrochloric acid molar concentrations in the retentate side and $\overline{C_{Fe,mol}^D}$ and $\overline{C_{HCl,mol}^D}$ in the

16   diffusate side, $U_{ZnCl_2}^{FeCl_2}$ and $U_{ZnCl_2}^{HCl}$ are the secondary overall mass transfer coefficients to take into

17   account the passage of zinc due to the presence of the iron chlorides and the hydrochloric acid, P_{Zn}

1 is the membrane permeability to ZnCl₂. $U_{ZnCl_2}^{FeCl_2}$, $U_{ZnCl_2}^{HCl}$ and P_{Zn} were derived from focused

2 experiments carried out at the laboratory scale (Gueccia et al., 2019b).

3 P_{Zn} can be evaluated as follows

$$P_{Zn} = -9.59 \cdot 10^{-3} \cdot \overline{C_{Zn}^2} + 6.19 \cdot 10^{-3} \cdot \overline{C_{Zn}} + 2.60 \cdot 10^{-5} \tag{19}$$

4 in which, $\overline{C_{Zn}}$ is the average zinc mass concentration within the DD unit.

5 $U_{ZnCl_2}^{FeCl_2}$ and $U_{ZnCl_2}^{HCl}$ can be quantified as reported in the following equations 20-21:

$$U_{ZnCl_2}^{FeCl_2} = 1.51 \cdot 10^{-6} \cdot \overline{C_{Zn}^2} + 3.88 \cdot 10^{-7} \cdot \overline{C_{Zn}} + 6.20 \cdot 10^{-8} \tag{20}$$

$$U_{ZnCl_2}^{HCl} = -1.73 \cdot 10^{-6} \cdot \overline{C_{Zn}^2} + 1.10 \cdot 10^{-6} \cdot \overline{C_{Zn}} + 2.44 \cdot 10^{-8} \tag{21}$$

6 For the water passage two contributions are considered: the osmotic and the drag fluxes through the

7 membrane, where the latter is related to the water solvation shell of transported acid. The osmotic

8 flux J_{os} is calculated by Eq. 22.

$$J_{os} = 3,600 \cdot P_{os} \cdot \Delta \pi \tag{22}$$

9 where P_{os} is the water permeability, $\Delta \pi$ is the average osmotic pressure difference between the two

10 solutions. The expression for P_{os} was derived experimentally (Gueccia et al., 2019b):

$$P_{os} = 1.26 \cdot 10^{-7} \cdot \overline{C_{HCl,mol}^R}^2 - 9.04 \cdot 10^{-7} \cdot \overline{C_{HCl,mol}^R} + 8.13 \cdot 10^{-6} \tag{23}$$

11 in which $\overline{C_{HCl,mol}^R}$ is the average hydrochloric acid molar concentration in the retentate side of the

12 DD unit.

$$\pi = \frac{R \, T \, MM_w \phi}{1000 v_w} \cdot \sum i m_i \tag{24}$$

13 where π is the osmotic pressure, R is the gas constant, T the average temperature, MM_w is the solvent

14 molecular weight, v_w is the molar volume of the solvent, i is the Van't Hoff coefficient and m_i is the

1   molality of the i-component. The osmotic coefficient ϕ was derived following the Pitzer multi-ionic

2   virial equations (Pitzer et al., 1977).

3   The drag flux J_{drag} is calculated according to the following equation:

$$J_{drag} = \left(7 \cdot \frac{w_{HCl}^{DD}}{MM_{HCl}} + 18 \cdot \frac{w_{FeCl_2}^{DD}}{MM_{FeCl_2}} + 18 \frac{w_{ZnCl_2}^{DD}}{MM_{ZnCl_2}} \right) \cdot MM_{H_2O} \tag{25}$$

4   where $w_{HCl}^{DD}, w_{FeCl_2}^{DD}$ and $w_{ZnCl_2}^{DD}$ are the HCl, FeCl$_2$ and ZnCl$_2$ mass flow rates passing through the DD

5   membrane, $MM_{HCl}, MM_{H_2O}, MM_{FeCl_2}$ and MM_{ZnCl_2} are the HCl, H$_2$O, FeCl$_2$ and ZnCl$_2$ molar masses.

6   The local ΔC driving force in terms of HCl concentration difference between retentate and diffusate

7   streams in the DD unit is bound to be higher than 3 g l^{-1}. Finally, the overall mass balance and the

8   generic i-component mass balance for the DD unit are reported in Eqs. 26 and 27

$$w^{DS} + w^{WAS} = w^{MRB} + w^{RAS} \tag{26}$$

$$w_i^{DS} + w_i^{WAS} = w_i^{MRB} + w_i^{RAS} \tag{27}$$

9   where w^{DS}, w^{WAS}, w^{MRB} and w^{RAS} are the total mass flow rates of the *Draw Solution*, *Waste Acid*

10   *Solution*, *Metals Rich Brine* and *Recovered Acid Solution* streams, while the subscript *i* indicates the

11   i-component (e.g. FeCl$_2$, HCl, ZnCl$_2$). The main figure of merit to assess the Diffusion Dialysis

12   performance is the Recovery Ratio of acid (RR), which is defined as follows

$$RR\ (\%) = \frac{w_{HCl}^{RAS} - w_{HCl}^{DS}}{w_{HCl}^{WAS}} \cdot 100 \tag{28}$$

13   where w_{HCl}^{RAS}, w_{HCl}^{DS} and w_{HCl}^{WAS} are the hydrochloric acid mass flow rate of the RAS, DS and WAS

14   solutions, respectively.

15   **3.3 Membrane Distillation unit**

16   With regard to Membrane Distillation unit, the streams considered for the simulation are: *Recovered*

17   *Acid Solution* as inlet, *Recovered Pickling Solution* and *Permeate* as outlets (see Figure 7).
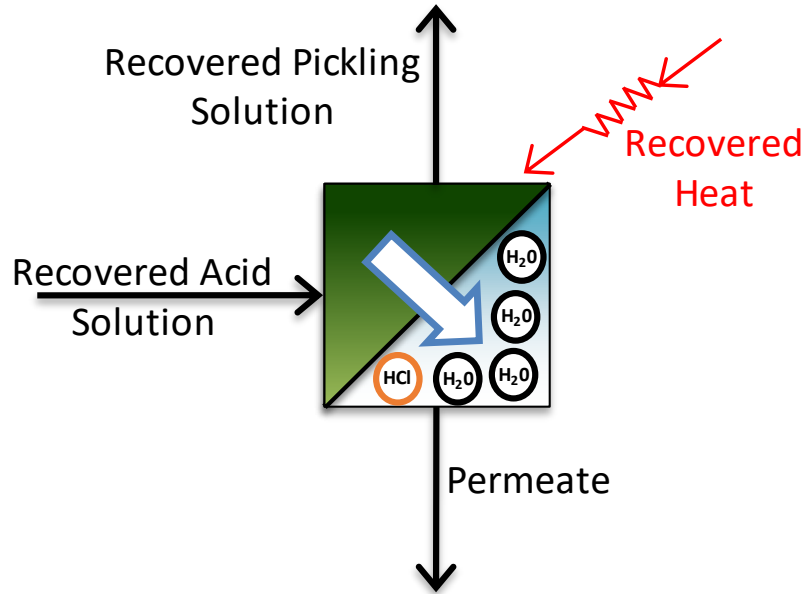
Figure 7. Membrane Distillation process scheme.

The fluxes of water and HCl in the vapour phase passed through the membrane are derived from simulations carried out by another research partner within the ReWaCEM consortium (Winter D., 2014). The values of J_i used in the model are extrapolated from simulations results carried out considering fixed temperature values at both the sides of the membrane. Specifically, in the range of the considered concentrations, and fixing average temperature to 75-65 °C, the fluxes are calculated to be: J_w=2.97-3.02 kg m^{-2} h^{-1} and J_{HCl}= 0.08-0.12 kg m^{-2} h^{-1}, for HCl concentration entering with the *Recovered Acid Solution* varying from 75 to 111 g l^{-1}.

The overall and for the i-component mass balances for the Membrane Distillation unit are reported in Eqs. 29 and 30:

$$w^{RAS} = w^{RPS} + w^{Perm} \tag{29}$$

$$w_i^{RAS} = w_i^{RPS} + w_i^{Perm} \tag{30}$$

where w^{RAS}, w^{RPS} and w^{Perm} are the total mass flow rates of the *Recovered Acid Solution*, *Recovered Pickling Solution* and Membrane Distillation *Permeate* streams.

1 The efficiency of the MD unit can be evaluated according to the Concentration Ratio parameter (CR)

2 given by

$$CR = \frac{C_{HCl}^{RPS}}{C_{HCl}^{RAS}}$$
(31)

3 which is the hydrochloric acid mass concentration ratio in the *Recovered Pickling Solution* C_{HCl}^{RPS} and

4 in the *Recovered Acid Solution* C_{HCl}^{RAS}.

5 **3.4 Reactive Precipitation stage**

6 The streams of the Reactive Precipitation unit, as shown in Figure 8, are: *Metal Rich Brine* and

7 *Oxidizing reactant* and *Alkaline reactant* streams as inlets, *Metal Sludge* and *Outlet Reactive*

8 *Precipitator* stream as outlets.
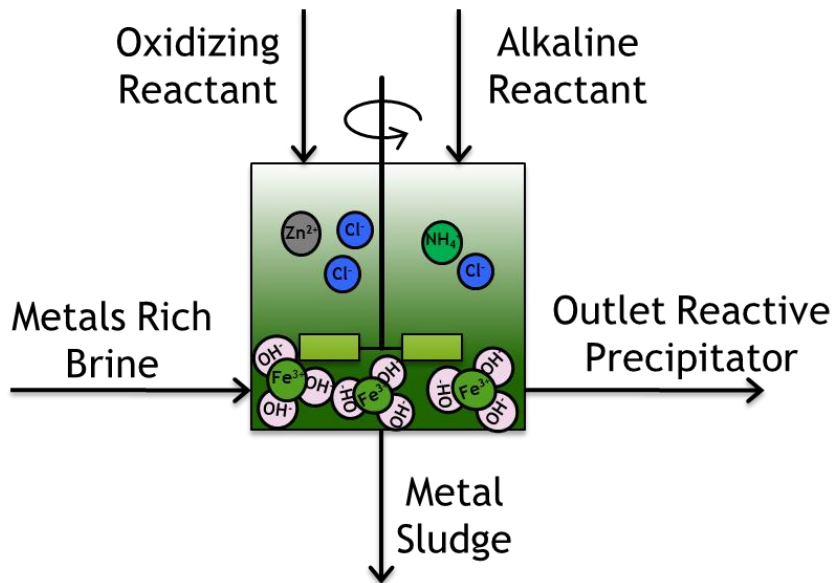
9

10 **Figure 8.** Reactive precipitator process scheme.

11 Also this unit is considered as a CSTR. The following reactions are considered in the reactive

12 precipitation process:

$$2FeCl_2 + H_2O_2 + 2HCl = 2FeCl_3 + 2H_2O$$
(32)
$$NH_4OH + HCl = NH_4Cl + H_2O$$
(33)
$$FeCl_3 + 3NH_4OH = Fe(OH)_3 + 3NH_4Cl$$
(34)

21

1   The hydrogen peroxide mass flow rate is calculated according to the following expression:

$$w_{H_2O_2}^{Ox} = \frac{w_{Fe}^{MRB} MM_{H_2O_2}}{2\,MM_{Fe}} \tag{35}$$

2   where $w_{H_2O_2}^{Ox}$ is the inlet H_2O_2 mass flow rate, w_{Fe}^{MRB} is the Fe mass flow rate in the MRB, $MM_{H_2O_2}$

3   and MM_{Fe} are the molar masses of H_2O_2 and Fe, respectively.

4   The mass flow rate of the alkaline reactant is computed using the relation:

$$w_{NH_4OH}^{alk} = \left[(10^{-pH_{in}} - 10^{-pH_{out}}) \cdot F^{MRB} + 2 \cdot \frac{C_{Fe}^{MRB} \cdot F^{MRB}}{MM_{Fe}}\right] \cdot 10^{-3} \cdot MM_{NH_4OH} \tag{36}$$

5   where $w_{NH_4OH}^{alk}$ is the NH_4OH mass flow rate in the alkaline reactant stream, pH_{in} and pH_{out} are the

6   inlet and outlet pH of the solution, F^{MRB} is the MRB volumetric flow rate, C_{Fe}^{MRB} is the iron molar

7   concentration, MM_{Fe} and MM_{NH_4OH} are the iron and NH_4OH molar masses, respectively.

8   Regarding the *Metal Sludge (MS)* calculations, the following equations are used:

$$w_{H_2O}^{MS} = \big[(10^{-pH_{in}} - 10^{-pH_{out}}) \cdot F^{MRB} \cdot 10^{-3} \cdot MM_{H_2O} + w_{H_2O}^{MRB} + w_{H_2O}^{alk} \\ + w_{H_2O}^{Ox}\big] \cdot \alpha \tag{37}$$

$$w_{HCl}^{MS} = [w_{HCl}^{MRB} - (10^{-pH_{in}} - 10^{-pH_{out}}) \cdot F^{MRB} \cdot 10^{-3} \cdot MM_{HCl}] \cdot \alpha \tag{38}$$

$$w_{Cl}^{MS} = [w_{Cl}^{MRB} + (10^{-pH_{in}} - 10^{-pH_{out}}) \cdot F^{MRB} \cdot 10^{-3} \cdot MM_{Cl}] \cdot \alpha \tag{39}$$

$$w_{NH_4}^{MS} = w_{NH_4OH}^{alk} \cdot \alpha \cdot \frac{MM_{NH_4}}{MM_{NH_4OH}} \tag{40}$$

$$w_{OH}^{MS} = \frac{2 \cdot 10^{-3} \cdot C_{Fe}^{MRB} \cdot F^{MRB} \cdot MM_{OH}}{MM_{Fe}} + \frac{2 \cdot w_{H_2O_2}^{Ox} \cdot MM_{OH}}{MM_{H_2O_2}} \tag{41}$$

9   where $w_{H_2O}^{MS}$, $w_{H_2O}^{MRB}$, $w_{H_2O}^{alk}$ and $w_{H_2O}^{Ox}$, w_{HCl}^{MS} and w_{HCl}^{MRB}, w_{Cl}^{MS} and w_{Cl}^{MRB}, $w_{NH_4}^{MS}$ and $w_{NH_4OH}^{alk}$, w_{OH}^{MS} and

10     $w_{H_2O_2}^{Ox}$ are the mass flow rates of water, HCl, chloride ions, ammonium cations, ammonium

11   hydroxide, hydroxyl ions and hydrogen peroxide in the *Metal Sludge*, *Metals Rich Brin*e, *Alkaline*

12   *reactant* and *Oxidizing reactant* streams; pH_{in} and pH_{out} are the inlet and outlet pH of the solution;

13   F^{MRB} is the MRB volumetric flow rate; MM_{H_2O}, MM_{HCl}, $MM_{Cl,}$ MM_{NH_4}, MM_{NH_4OH}, MM_{OH}, MM_{Fe}

14   and $MM_{H_2O_2}$ are the molar masses and C_{Fe}^{MRB} is the iron concentration in *Metals Rich Brin*e.

1   α is a coefficient which represents the amount of the flow rate of solution trapped in the humid cake,

2   expressed by the following equation:

$$\alpha = \frac{w_{sol}^{MS}}{w_{sol}^{MS} + w^{ORP}} \tag{42}$$

3   in which w^{ORP} is the *Outlet Reactive Precipitator* stream mass flow rate and w_{sol}^{MS} is the mass flow

4   rate of aqueous solution in the *Metal Sludge*. w_{sol}^{MS} is given by

$$w_{sol}^{MS} = w^{MS} - w_{prec}^{MS} \tag{43}$$

5   where w_{prec}^{MS} is the iron hydroxide mass flow rate precipitated within the reactive precipitation unit.

6   In this work, α was determined experimentally by precipitation and filtration tests and it was fixed

7   equal to 0.35.

8   Regarding the *Outlet Reactive Precipitator* stream, the pH is kept constant and equal to 4. The mass

9   flow rates of each i-component (i.e. H_2O, HCl, Cl^-, NH_4^+) can be calculated by the following

10   equation:

$$w_i^{ORP} = \frac{w_i^{MS}}{\alpha} \cdot (1 - \alpha) \tag{44}$$

11

12   3.5 Brine Membrane Distillation unit

13   Regarding the Brine MD, the streams to be characterized are: *Outlet Reactive Precipitator* stream as

14   inlet and *Fluxing Solution* and *Distillate* as outlets (see Figure 9).

Distillate

Outlet reactive precipitator

Recovered Heat

Fluxing Solution
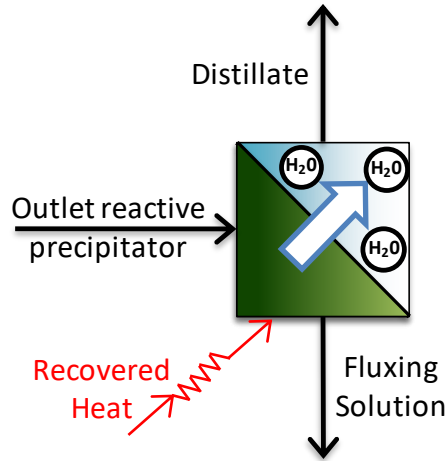
Figure 9. Brine Membrane Distillation process scheme.

The Brine MD is designed considering that a maximum allowable ammonium chloride concentration

of 350 g l^{-1} in the MD outlet stream is permitted due to the salt solubility limit.

The overall and for the i-component mass balance for the Membrane Distillation unit are reported in

Eqs. 45 and 46:

$$w^{ORP} = w^{Dist} + w^{FS} \tag{45}$$

$$w_i^{ORP} = w_i^{Dist} + w_i^{FS} \tag{46}$$

where w^{ORP}, w^{Dist} and w^{FS} are the total mass flow rates of the *Outlet Reactive Precipitator* solution,

Distillate and *Fluxing Solution* streams.

The equations presented in paragraph 3 are solved using Microsoft® Office Excel spreadsheets with

macros, according to the numerical algorithm shown in Figure 10. By selecting the C_{HCl}^{WAS} value and

assuming a first guess value for *RR* and DD and MD membrane areas, the mass balance equations

for the pickling, DD and MD units are solved. Computed results lead to the estimation of operating

parameters, which should verify the constraints reported in the rhombic shapes. If not, DD and MD

area and *RR* are adjusted to achieve this goal. When these conditions are fully satisfied, mass balances

of Reactive Precipitation and Brine MD units are solved. Then, the $C_{NH_4Cl}^{FS}$ value is checked to be

24

1   equal to 350 g l⁻¹. If not, Brine MD area is varied to obtain the fixed value and the numerical

2   procedure is completed.

3
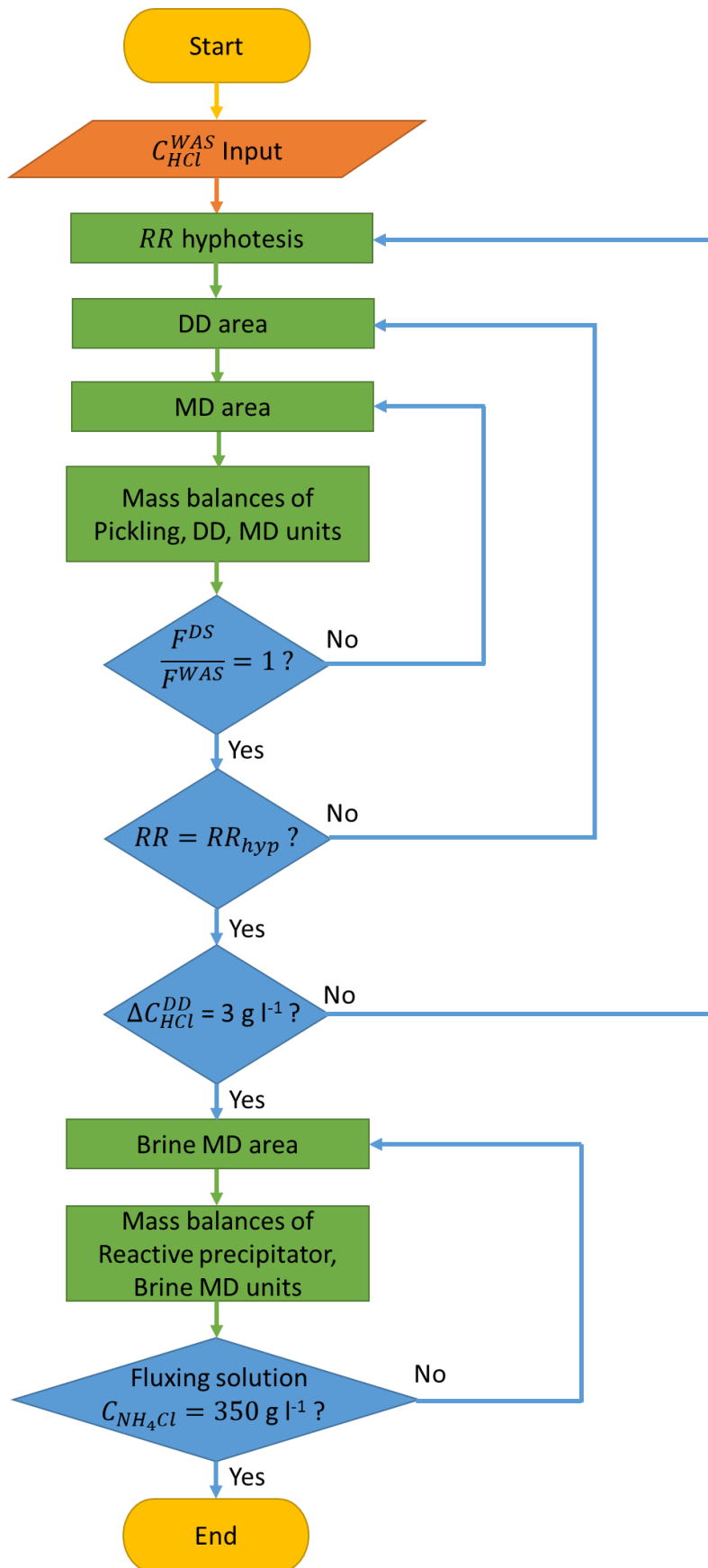
Figure 10.

Figure 10. The implemented algorithm solved within Microsoft® Office Excel spreadsheets with macros.

4. Results and discussion

A parametric analysis of the process was performed by varying the main operating parameters in order to find the operating conditions for optimal process efficiency. In particular, three case-studies were considered by fixing the HCl concentration in the pickling bath to 80, 100 and 120 g l^{-1} and imposing the corresponding iron concentration from the Kleingarn curve. It is worth noting that values of evaporation flux and inlet/outlet entrainment rate in the pickling tank were considered constant (as reported in Table 1) for the three analysed scenarios.

As a reference case, the streams reported in the process flow diagram of Figure 3 were characterized considering the HCl concentration in the pickling bath equal to 100 g l^{-1}. The relevant streams properties are reported in Table 3.

Table 3. PFD streams characterization (see Figure 3) for C_{HCl}^{WAS}=100 g l^{-1}

Stream	w	F	C_{HCl}	$C_{Fe^{2+}}$	$C_{Zn^{2+}}$	C_{NH_4Cl}	C_{NH_4OH}	$C_{H_2O_2}$
	kg h^{-1}	l h^{-1}	g l^{-1}	g l^{-1}	g l^{-1}	g l^{-1}	g l^{-1}	g l^{-1}
A1	21.1	16.4	100	117	12.6	0.0	0.0	0.0
A2	19.3	16.0	14.4	102	4.77	0.0	0.0	0.0
A3	5.44	5.40	22.8	0.0	0.0	0.0	0.0	0.0
A4	16.4	16.4	7.5	0.0	0.0	0.0	0.0	0.0
A5	18.3	16.8	91.3	16.6	7.81	0.0	0.0	0.0
A6	12.9	11.4	124	24.4	11.5	0.0	0.0	0.0
A7	15.7	15.1	0.00252	0.0	3.30	154	0.0	0.0
A8	7.28	6.60	0.00574	0.0	7.52	350	0.0	0.0
A9	8.31	8.31	0.0	0.0	0.0	0.0	0.0	0.0
A10	11.0	11.0	0.0	0.0	0.0	0.0	0.0	0.0
A11	11.6*	-	-	-	-	-	-	-
A12	3.44	3.07	0.0	0.0	0.0	0.0	0.0	325
A13	4.63	5.20	0.0	0.0	0.0	0.0	525	0.0
A14	7.32	6.26	400	0.0	0.0	0.0	0.0	0.0

*Metal sludge, after filtration, containing 29% iron(III) hydroxide and 71% of spent brine with up to 13% of ZnCl$_2$ and NH$_4$Cl salts).

1   Clearly, the variation of HCl and Fe concentration in the pickling bath affects flow rates, composition

2   and performance parameters of the integrated system.

3   Figure 11 shows the volume flow rates of all considered streams. They strongly depend on the HCl

4   concentration. In fact, as shown in equation 8, the *WAS* flow rate is inversely proportional to the iron

5   concentration. Moreover, the iron and hydrochloric acid concentrations are interrelated by the equation

6   9 (the Kleingarn curve). Thus, the higher the hydrochloric acid concentration, the lower the iron

7   concentrations. As a consequence, the increase of C_{HCl}^{WAS} leads to the rise of the *WAS* flow rate. Of course,

8   the higher the *WAS* flow rate, the higher that of the other process streams.
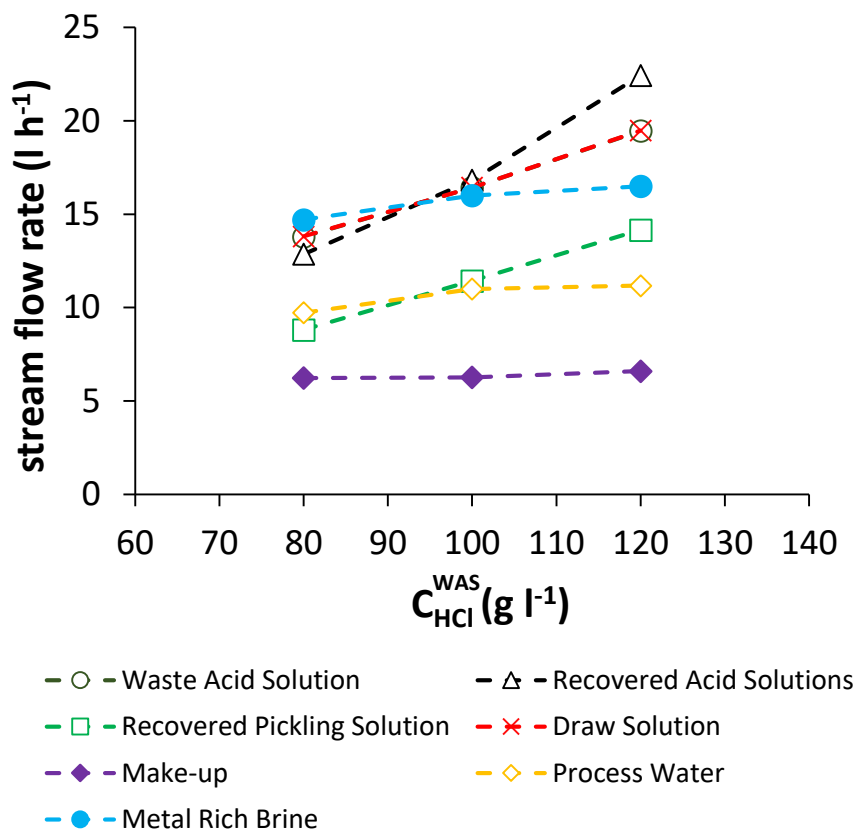
**Figure 11.** Streams flow rates as a function of C_{HCl}^{WAS}.

11   The HCl concentration in the *WAS* affects acid and iron concentrations of the other streams, such as

12   *RPS*, *RAS* and *MRB*. In fact, as shown in Figure 12, increasing HCl concentration from 80 to 120 g l^{-1}

13   leads to an increase of acid and a reduction of iron concentrations in the just mentioned streams.

27
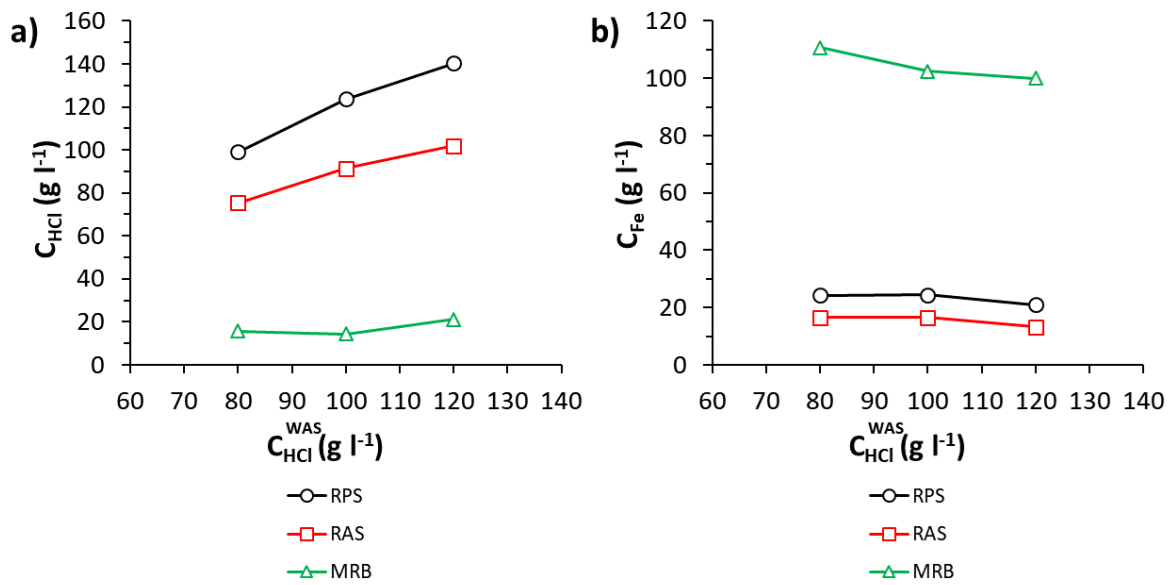
1

2   **Figure 12.** HCl concentrations a) and Iron concentrations b) in the *RPS*, *RAS* and *MRB* as a function of

3   C_{HCl}^{WAS}.

4   The hydrochloric acid recovery performance from the pickling waste is given by the DD Recovery Ratio

5   and the MD Concentration Ratio, shown in Figure 13.
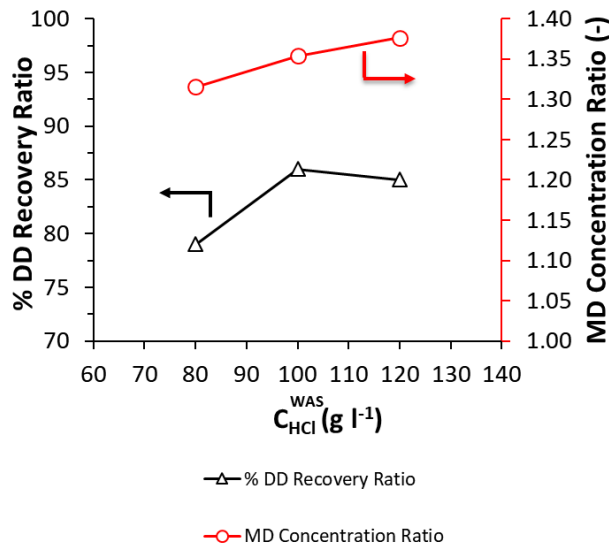
6

7   **Figure 13.** DD Recovery Ratio and MD Concentration Ratio as function of C_{HCl}^{WAS}.

8   The integrated system allows an average DD Recovery Ratio higher than 80%. Moreover, high acid

9   concentrations of the *RPS* (MD outlet) are obtained because of the high Concentration Ratio values of

28

1 the MD unit (i.e. 1.35 on average). Thereby, the *Recovered Pickling Solution* can be effectively

2 recirculated and re-used in the pickling bath.

3 Concerning the reactive precipitation unit, the inlet and outlet streams flow rates are shown in Table 4.

4 **Table 4.** Oxidizing reactant, Alkaline reactant and Iron Hydroxide streams flow rates as function of
5 C_{HCl}^{WAS}.
6

C_{HCl}^{WAS} (g l^{-1})	80	100	120
Oxidizing reactant (kg h^{-1})	3.41	3.44	3.46
Alkaline reactant (kg h^{-1})	3.83	4.63	4.08
Iron Hydroxide (kg h^{-1})	3.11	3.16	3.13

7

8 The flow rates of the *Oxidizing reactant* solution and of the Iron Hydroxide are poorly dependent on the

9 C_{HCl}^{WAS}, while an increasing-decreasing trend was found for the *Alkaline reactant* solution. The average

10 *Oxidizing* and *Alkaline* reactants flow rates are 3.4 and 4.2 kg h^{-1}, respectively. Consequently, an Iron

11 Hydroxide stream of 3.2 kg h^{-1} is obtained with high purity (i.e. >99.5%). Such product results in an

12 economic benefit for the company since it represents a marketable product with significant added value.

13 As a result of the circular approach here adopted, the process water is basically provided by the Brine

14 MD unit as reported in Figure 14, where the water consumption of the integrated process is analyzed.

15 In fact, the Brine MD *Distillate* stream is recirculated according to the scheme in Figure 3, where the

16 *Distillate* is part of the *Draw Solution* in the inlet side of DD unit. *Distillate* stream shows an average

17 flow rate of 10.6 kg h^{-1}, thus representing more than 70% of the inlet process water of the integrated

18 system.

19
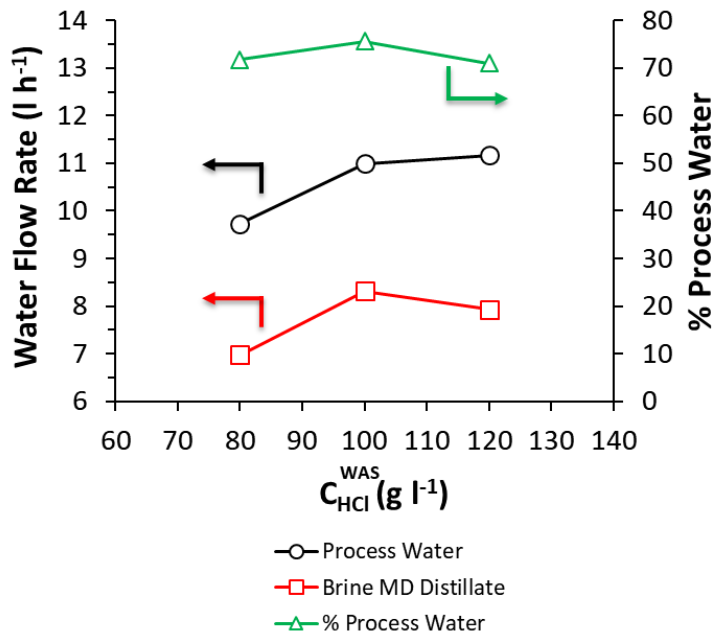
Figure 14. *Process Water* and Brine MD *Distillate* (left axis) and % Process Water recovered by the Brine MD *Distillate* (right axis) as function of C_{HCl}^{WAS}.

Likewise, the outlet stream in the feed side of the Brine MD is re-used in the fluxing step of the hot-dip galvanizing plant. This fact ensures the resources circularity strategy and the total elimination of the waste.

For what concerns the pickling bath, as stated above, it operates in continuous (i.e. the steady-state assumption) maintaining the optimal concentrations. This allows the minimization of the processing time.

According to Kleingarn, the pickling time is a function of the hydrochloric acid and iron chlorides mass fractions. In particular, in the optimal conditions represented by the Kleingarn curve (Figure 2), the higher the hydrochloric acid mass fraction, the lower the pickling time. This trend is reported in Figure 15. In the studied range of HCl concentration, process time diminishes from 7.6 min at 80 g l^{-1} to 5.2 min at 120 g l^{-1}, in an almost linear shape, thereby resulting in a 32% of reduction. This fact leads to a considerable decrease in the operators' labor cost.
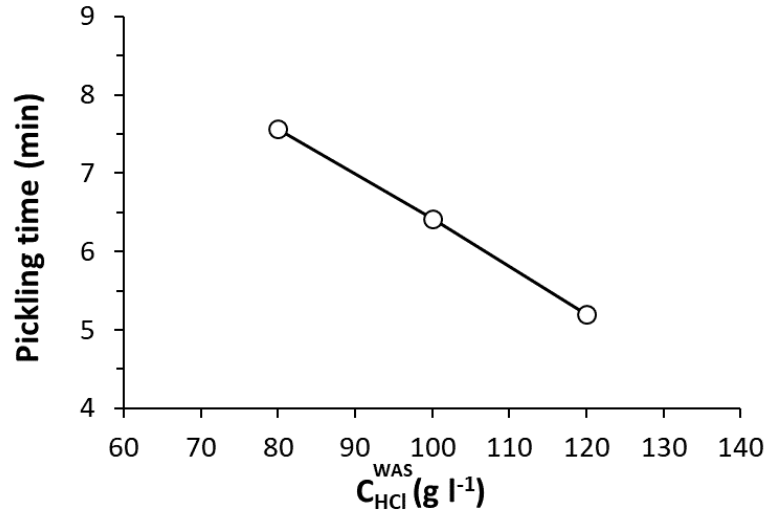
1

2 **Figure 15.** Theoretical pickling time as a function of the hydrochloric acid concentration in the
3 Kleingarn optimal conditions (derived from (Kleingarn, 1988).

4 Finally, a preliminary economic investigation was carried out to evaluate the economic profitability due

5 to the introduction of the integrated system in the hot-dip galvanizing plant. Specifically, a simplified

6 profitability analysis was performed estimating three important indexes: (i) Net Present Value (NPV),

7 (ii) Discounted Payback Period (DPBP) and (iii) Discounted Cash Flow Rate Of Return (DCFROR).

8 The economic analysis was developed following a well-known procedure described elsewhere (Turton,

9 2012). The inputs are reported in Table 5.

10 **Table 5.** Economic model input
11

Working hours	1,920 h/y
Project life time	5 years
Interest rate	4%
Taxation rate	33%

12

13 Capital costs were calculated as Total Module Cost (Table 6), which include all direct, indirect,

14 contingency and fee costs (Turton, 2012) (i.e. all costs from equipment purchase to plant start-up).

15 **Table 6.** Capital costs input
16

	Total Module cost
Pre-treatment unit	10,600 €
Reactive precipitation unit	10,400 €

Heat-exchanger	7,800 €	
Pumps	15,500 €	
Membrane units	15,300 €	

The membrane units module costs were preliminarily estimated on the basis of data provided by another

research partner within the ReWaCEM consortium.

The manufacturing costs consist of (i) Direct Costs, (ii) Fixed Manufacturing Costs and (iii) General

Manufacturing Expenses (Turton, 2012). Manufacturing costs are reported in Table 7.

Table 7. Manufacturing costs input

	Unitary cost	Flow rate
Alkaline reactant	$0.55 \, €\,l^{-1}$	$6.64 \, l\,h^{-1}$
Oxidizing reactant	$0.38 \, €\,kg^{-1}$	$3.92 \, l\,h^{-1}$
HCl Make-up	$0.125 \, €\,kg^{-1}$	$2.56 \, kg\,h^{-1}$
Process water	$0.95 \, €\,m^{-3}$	$0.85 \, l\,h^{-1}$

Moreover, a taxation of 33% and an interest rate of 4% were adopted.

In addition, the simple straight-line depreciation method was applied. This was chosen because it

determines minor savings compared to other depreciation methodologies therefore resulting in a more

conservative economic estimate.

Revenues considered in this analysis concern the selling of products, the saving of waste acid disposal

cost and the gain due to the increased manufactured steel flow rate (see Table 8).

Table 8. Revenues input

	Unitary revenue	Flow rate
Iron(III) hydroxide	$5 \, €\,kg^{-1}$	$4.0 \, kg\,h^{-1}$
Fluxing solution	$0.1 \, €\,kg^{-1}$	$9.3 \, kg\,h^{-1}$
Saving of waste acid disposal	$160 \, €\,ton^{-1}$	$9.7 \, kg\,h^{-1}$
Added value of enhanced production	$45 \, €\,ton^{-1}$	$80 \, kg\,h^{-1}$

Based on a project life time of five years, the NPV, DPBP and DCFROR were computed and reported

in Table 9.

Table 9. Profitability indexes

1

NPV	35,500 €
DPBP	3.1 years
DCFROR	23.6 %

2

3   As shown in Table 9 the NPV is found equal to 35,500 €, thus indicating that the adoption of the recovery

4   integrated process in the current pickling process can be profitable for the company.

5   Moreover, even considering higher capital costs due to the uncertainty estimation of the membrane units,

6   the Fixed Capital Investment should be higher than 88,000 € to make the process unprofitable. It is

7   worth noting that this preliminary economic analysis was performed for the pilot plant. However, taking

8   into account the economy of scale, the scale-up of the pilot plant would further increase the profit

9   margin.

10   Thus, the integrated system not only allows to implement a sustainable integrated resources cycle but

11   also to obtain an economic return, which is attractive in the hot-dip galvanizing industry. This

12   preliminary economic analysis will be further developed in the future in order to get a more detailed

13   estimate of the process profitability.

14   **5. Conclusions**

15   In the present work, a novel membrane-integrated waste acid recovery process from pickling solutions

16   based on circular economy is proposed and investigated. In order to do so, a process simulator was

17   developed. The proposed integrated process guarantees a pickling continuous operation under optimal

18   conditions, thus avoiding the standard periodic steps of withdrawing and refilling pickling baths, being

19   one of the major environmental and economic drawbacks of the process.

20   The parametric analysis carried out showed the effect of increasing the inlet hydrochloric acid

21   concentration in the *Waste Acid Solution* on the main process streams. Main operative parameters were

22   monitored, including HCl and Fe concentrations, performance indicators and membrane area

23   requirements. A high acid recovery (higher than 79%) was obtained in the DD, while keeping a low iron

24   leakage. Moreover, the acid solution concentration step was effectively achieved in the MD unit, where

1 the feed solution is concentrated in HCl of 35%. The continuous operation of the integrated system

2 allowed pickling to be performed under optimal conditions, thus reducing the pickling time and enhance

3 the overall system efficiency.

4 Finally, a preliminary economic analysis was performed and collected results indicated that the process

5 proposed is profitable under the selected conditions.

6 **Acknowledgments**

11 **Acronyms**

AEM	Anion Exchange Membrane
CSTR	Continuous-flow Stirring Tank Reactor
DD	Diffusion Dialysis
DS	Draw Solution
FS	Fluxing Solution
MD	Membrane Distillation
MRB	Metals Rich Brine
MS	Metal Sludge
MU	Make-up
ORP	Outlet Reactive Precipitator
PFD	Process Flow Diagram
PW	Process Water
RAS	Recovered Acid Solution
RPS	Recovered Pickling Solution
WAS	Waste Acid Solution

12 **Nomenclature**

A (m^2)	membrane area
C (g l^{-1})	mass concentration
CR (-)	concentration ratio
F (l h^{-1})	volumetric flow rate
i (-)	Van't Hoff coefficient
J (kg h^{-1} m^{-2})	mass flux
k (kg h^{-1} ton^{-1})	kinetic constant
m (mol kg^{-1})	molality
m_s (ton)	manufactured steel mass

MM (g mol^{-1})   molar mass
N_{hours} (-)   number of yearly working hours
P (m h^{-1})   membrane permeability
P_{os} (l bar^{-1} m^{-2} s^{-1})   osmotic permeability
pH pH value
R (l bar K^{-1} mol^{-1})   gas constant
RR recovery ratio
T (K)   temperature
U (m s^{-1})   secondary overall mass transfer coefficient
w (kg h^{-1})   mass flow rate of the integrated process streams
w_y (ton y^{-1})   mass flow rate of the actual Tecnozinco plant streams

1   *Greek letters*

α (-)   amount of the flow rate of solution trapped in the humid cake
v (l mol^{-1})   molar volume
Δ (-)   difference of value
π (bar)   osmotic pressure
ρ (kg m^{-3})   mass density
ϕ (-)   osmotic coefficient

2   *Superscripts*

alk alkaline
D diffusion dialysis diffusate
$Dist$ distillate
DD diffusion dialysis
DS draw solution
$entr, in$ entrainment stream, inlet
$entr, out$ entrainment stream, outlet
$evap$ evaporating stream
FS fluxing solution
gas gaseous emission
MRB metals rich brine
MS metal sludge
MU make-up
ORP outlet reactive precipitator
Ox Oxidant
$Perm$ permeate
pw process water
R diffusion dialysis retentate
RAS recovered acid solution
$Rinsing$ rinsing solution
RPS recovered pickling solution
WAS waste acid solution in the integrated process
$waste$ actual waste produced in Tecnozinco plant

3   *Subscripts*

d diffusate stream of the DD unit
$drag$ water molecules dragged by the acid through the membrane in DD
$evap$ evaporating stream
i i-component

35

in	inlet
mol	molar concentrations
os	osmotic flux
out	outlet
oxides	oxides and elementary iron
prec	precipitated
r	retentate stream of the DD unit
sol	aqueous solution
w	water

1 **References**

2 Bascone, D., Cipollina, A., Morreale, M., Randazzo, S., Santoro, F., Micale, G., 2016. Simulation of

3   a regeneration plant for spent pickling solutions via spray roasting. Desalin. Water Treat.

4   https://doi.org/10.1080/19443994.2015.1137146

5 Campano, B.R., 2012. The Kleingarn regenerated spent acid at increasing ferrous and ferric chloride

6   content. Jeddah , Saudi Arabia.

7 Fresner, J., Schnitzer, H., Gwehenberger, G., Planasch, M., Brunner, C., Taferner, K., Mair, J., 2007.

8   Practical experiences with the implementation of the concept of zero emissions in the surface

9   treatment   industry   in   Austria.   J.   Clean.   Prod.   15,   1228-1239.

10   https://doi.org/10.1016/j.jclepro.2006.07.024

11 Gueccia, R., Randazzo, S., Martino, D.C., Cipollina, A., Micale, G., 2019a. Experimental

12   investigation and modeling of diffusion dialysis for HCl recovery from waste pickling solution.

13   J. Environ. Manage. 235, 202–212. https://doi.org/10.1016/j.jenvman.2019.01.028

14 Gueccia, R., Ruiz Aguirre Alba, Randazzo, S., Cipollina, A., Micale, G., 2019b. Diffusion dialysis

15   for HCl and heavy metals separation from highly concentrated pickling solutions. Submitted to

16   14th Conference on Sustainable Development of Energy, Water and Environment Systems, 01

17   - 04 October 2019, Dubrovnik, Croatia

18 Hernández-Betancur, J.D., Hernández, H.F., Ocampo-Carmona, L.M., 2019. A holistic framework

19   for assessing hot-dip galvanizing process sustainability. J. Clean. Prod. 206, 755-766.

20   https://doi.org/10.1016/j.jclepro.2018.09.177

Jatuphaksamphan, Y., Phinichka, N., Prapakorn, K., Supradist, M., 2010. Pickling Kinetics of Tertiary Oxide Scale Formed on Hot-Rolled Steel Strip. J. Met. Mater. Miner. 20, 33–39.

Jung Oh, S., Moon, S.H., Davis, T., 2000. Effects of metal ions on diffusion dialysis of inorganic acids. J. Memb. Sci. 169, 95–105. https://doi.org/10.1016/S0376-7388(99)00333-6

Kleingarn, J.P., 1988. Pickling in hydrochloric acid, in: Edited Proceedings: 15th International Galvanizing Conference. European General Galvanizers Association (EGGA); 1988. p. GF2/1–13.

Kong, G., White, R., 2010. Toward cleaner production of hot dip galvanizing industry in China. J. Clean. Prod. 18, 1092-1099. https://doi.org/10.1016/j.jclepro.2010.03.006

Laliberte, M., Cooper, W.E., 2004. Model for calculating the density of aqueous electrolyte solutions. J. Chem. Eng. Data 49, 1141–1151. https://doi.org/10.1021/je0498659

Leonzio, G., 2016. Recovery of metal sulphates and hydrochloric acid from spent pickling liquors. J. Clean. Prod. 129, 417–426. https://doi.org/10.1016/j.jclepro.2016.04.037

Liu, R., Qin, Y., Li, X., Liu, L., 2012. Concentrating aqueous hydrochloric acid by multiple-effect membrane distillation 6, 311–321. https://doi.org/10.1007/s11705-012-1207-3

Luo, J., Wu, C., Wu, Y., Xu, T., 2013. Diffusion dialysis of hydrochloric acid with their salts: Effect of co-existence metal ions. Sep. Purif. Technol. 118, 716–722. https://doi.org/10.1016/j.seppur.2013.08.014

Luo, J., Wu, C., Xu, T., Wu, Y., 2011. Diffusion dialysis-concept, principle and applications. J. Memb. Sci. https://doi.org/10.1016/j.memsci.2010.10.028

Machado, R.M., Gameiro, M.L.F., Rodrigues, J.M.A., Ismael, M.R.C., Reis, M.T.A., Carvalho, J.M.R., 2017. Recovery of hydrochloric acid from galvanizing industrial effluents. Sep. Sci. Technol. 52, 1333–1340. https://doi.org/10.1080/01496395.2017.1287193

Palatý, Z., Bendová, H., 2009. Separation of HCl + $FeCl_2$ mixture by anion-exchange membrane. Sep. Purif. Technol. https://doi.org/10.1016/j.seppur.2008.11.026

Palatý, Z., Žáková, A., 2006. Competitive transport of hydrochloric acid and zinc chloride through

polymeric anion-exchange membrane. J. Appl. Polym. Sci. 101, 1391–1397. https://doi.org/10.1002/app.22748

Pitzer K.S. and Kim J. J., Thermodynamics of Electrolytes. IV. Activity and Osmotic Coefficients for Mixed Electrolytes, J. Am. Chem. Soc., vol. 96, no. 18, 5701–5707, 1974

Regel-Rosocka, M., 2010. A review on methods of regeneration of spent pickling solutions from steel processing. J. Hazard. Mater. https://doi.org/10.1016/j.jhazmat.2009.12.043

Stocks, C., Wood, J., Guy, S., 2005. Minimisation and recycling of spent acid wastes from galvanizing plants. Resour. Conserv. Recycl. 44, 153–166. https://doi.org/10.1016/j.resconrec.2004.11.005

Tomaszewska, M., Gryta, M., Morawski, A.W., 2001. Recovery of hydrochloric acid from metal pickling solutions by membrane distillation. Sep. Purif. Technol. 22–23, 591–600. https://doi.org/10.1016/S1383-5866(00)00164-7

Tomaszewska, M., Gryta, M., Morawski, A.W., 1995. Study on the concentration of acids by membrane distillation 102, 113–122.

Turton, R., Bailie, R.C., Whiting, W.B., Shaeiwitz, J.A., Bhattacharyya, D., Analysis Synthesis and Design of Chemical Process, Prentice Hall, 2012

Winter, D., 2014. Membrane Distillation - a Thermodynamic, Technological and Economic Analysis, Dissertation submitted to the Department of Mechanical and Process Engineering of the University of Kaiserslautern, Germany, Unpublished results (www.reiner-lemoine-stiftung.de/stipendiaten/daniel-winter.html)

Xu, J., Lu, S., Fu, D., 2009. Recovery of hydrochloric acid from the waste acid solution by diffusion dialysis. J. Hazard. Mater. https://doi.org/10.1016/j.jhazmat.2008.10.064